








RESEARCH ARTICLE | MARCH 18 2025

Single molecule magnet's (SMM) effects on antiferromagnet-based magnetic tunnel junction

Special Collection: [16th Joint MMM-Intermag Conference](#)

Babu Ram Sankhi ; Erwan Peigney ; Hayden Brown ; Pius Suh ; Carlos Rojas-Dotti ;
 José Martínez-Lillo ; Pawan Tyagi 



AIP Advances 15, 035035 (2025)

<https://doi.org/10.1063/9.0000868>


Articles You May Be Interested In

Monte Carlo simulation to study the effect of molecular spin state on the spatio-temporal evolution of equilibrium magnetic properties of magnetic tunnel junction based molecular spintronics devices

AIP Advances (January 2021)

Impact of direct exchange coupling via the insulator on the magnetic tunnel junction based molecular spintronics devices with competing molecule induced inter-electrode coupling

AIP Advances (January 2021)

Magnetic force microscopy revealing long-range room temperature stable molecule bridge-induced magnetic ordering on magnetic tunnel junction (MTJ) pillars

AIP Advances (March 2025)

Single molecule magnet's (SMM) effects on antiferromagnet-based magnetic tunnel junction

Cite as: AIP Advances 15, 035035 (2025); doi: 10.1063/9.0000868

Submitted: 8 November 2024 • Accepted: 3 February 2025 •

Published Online: 18 March 2025



Babu Ram Sankhi,^{1,a)} Erwan Peigney,¹ Hayden Brown,¹ Pius Suh,¹ Carlos Rojas-Dotti,^{2,3} José Martínez-Lillo,² and Pawan Tyagi^{1,b)}

AFFILIATIONS

¹ Center for Nanotechnology Research and Education, Mechanical Engineering, University of District of Columbia, Washington, District of Columbia 20008, USA

² Departament de Química Inorgànica/Instituto de Ciencia Molecular (ICMol), University of Valencia, c/Catedrático José Beltrán 2, Paterna (Valencia) 46980, Spain

³ Área Química Inorgánica/Departamento Estrella Campos, Facultad de Química, Universidad de República, General Flores, 2124 Montevideo, Uruguay

Note: This paper was presented at the 16th Joint MMM-Intermag Conference.

a) Author to whom correspondence should be addressed: babu.sankhi@udc.edu

b) E-mail: ptyagi@udc.edu

ABSTRACT

Single-molecule magnets (SMMs) are pivotal in molecular spintronics, showing unique quantum behaviors that can advance spin-based technologies. By incorporating SMMs into magnetic tunnel junctions (MTJs), new possibilities emerge for low-power, energy-efficient data storage, memory devices and quantum computing. This study explores how SMMs influence spin-dependent transport in antiferromagnet-based MTJ molecular spintronic devices (MTJMSDs). We fabricated cross-junction MTJ devices with an antiferromagnetic Ta/FeMn bottom electrode and ferromagnetic NiFe/Ta top electrode, with a ~ 2 nm AlO_x layer, designed so that the AlO_x barrier thickness at the junction intersection matched the SMM length, allowing them to act as spin channels bridging the two electrodes. Following SMM treatment, the MTJMSDs exhibited significant current enhancement, reaching a peak of $40 \mu\text{A}$ at 400 mV at room temperature. In contrast, bare MTJ junctions experienced a sharp current reduction, falling to the pA range at 0°C and remaining stable at lower temperatures—a suppression notably greater than in SMM-treated samples (Ref: Sankhi *et al.*, Journal of Magnetism and Magnetic Materials, p. 172608, 2024). Additional vibration sample magnetometry on pillar shaped devices of same material stacks indicated a slight decrease in magnetic moment after incorporating SMMs, suggesting an effect on magnetic coupling of molecule with electrodes. Overall, this work highlights the promise of antiferromagnetic materials in optimizing MTJMSD devices and advancing molecular spintronics.

© 2025 Author(s). All article content, except where otherwise noted, is licensed under a Creative Commons Attribution (CC BY) license (<https://creativecommons.org/licenses/by/4.0/>). <https://doi.org/10.1063/9.0000868>

I. INTRODUCTION

Molecular spintronic devices (MSDs) which can exploit the spin properties of electrons, are appealing candidates for next-generation data storage and memory applications.^{1,2} These devices hold potential for uncovering novel quantum phenomena.^{3,4} Traditional MSD fabrication methods have demonstrated the practical viability of MSDs but face significant challenges, such as limitations

in scalability, the integration of magnetic electrodes, atomic-level defects, and potential damage to molecular channels during fabrication processes.^{5,6} To overcome these barriers and pave the way for commercially viable spintronic devices, magnetic tunnel junctions (MTJs) were introduced as an alternative design approximately two decades ago.⁶ These structures consist of top and bottom magnetic electrodes with exposed edges, separated by an insulating barrier (Fig. 1(a)). In this setup, molecules such as single-molecule magnets

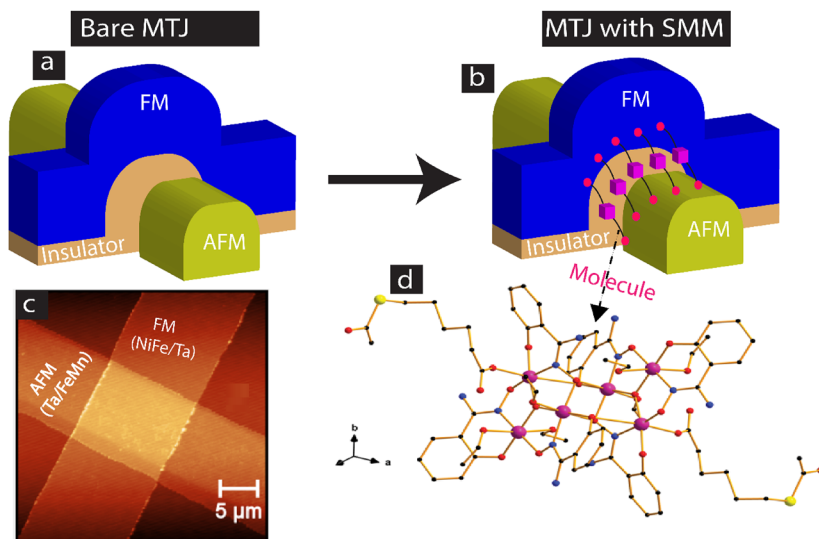


FIG. 1. Schematic of 3-D magnetic tunnel junction (MTJ) with exposed side edges (a) bare (b) with the single molecule magnet (SMM). (c) 2-D atomic force microscopy image of one junction of the bare MTJ showing bottom antiferromagnetic Ta/FeMn and top ferromagnetic NiFe/Ta electrodes (d) SMM's chemical structure.¹⁹

(SMMs) and organometallic molecular clusters (OMCs) can bridge the electrodes, forming a magnetic tunnel junction-based molecular spintronic device (MTJMSD) with a molecular spin channel (Fig. 1(b)).

The single-molecule magnet (SMM) we used in our experiment was Mn_6 ,^{7,8} which consists of six manganese ions bridged by organic ligands that form a specific geometric arrangement as shown in Fig. 1(d). These organic ligands, along with the molecular orbital structure, block charge carrier movement, resulting Mn_6 as an insulating material. Despite their insulating nature, Mn_6 SMMs exhibit fascinating magnetic properties. They have spin ground states of $S = 4$ and $S = 12$, along with significant magnetic anisotropy.⁹ This anisotropy creates an energy barrier that prevents the reversal of magnetization, which is crucial for maintaining a stable magnetic moment at low temperatures. Additionally, these SMMs exhibit quantum tunneling of magnetization, a unique quantum property that further highlights their potential for advanced technological applications.^{4,7,10}

Various experimental and theoretical studies have investigated the novel magnetic behavior arising from the coupling of organic molecules with ferromagnetic electrodes.^{11–15} For instance, a study of ferromagnet-based MTJMSDs using SMMs observed a notable spin solar cell effect in these structures.¹⁶ One such SMM used in these studies, a complex with the chemical structure $[\text{Mn}_6(\mu_3\text{-O})_2(\text{H}_2\text{N-sao})_6(6\text{-atha})_2(\text{EtOH})_6]$ (where $\text{H}_2\text{N-saoH}$ = salicylamidoxime and 6-atha = 6-acetylthiohexanoate), includes thiol groups that form stable covalent bonds with magnetic electrodes, enhancing molecular integration in MTJs. Furthermore, previous simulation studies suggest that MTJMSDs composed of ferromagnetic (FM) and antiferromagnetic (AFM) electrode combinations, may exhibit a wide range of multistate magnetoresistance,¹⁷ highlighting the potential of these devices for high density data storage applications.¹⁸ Inspired by these findings, we fabricated an MTJ with a ferromagnetic (FM) NiFe top electrode and an antiferromagnetic (AFM) FeMn bottom electrode, as illustrated in the schematic (Fig. 1(a)). By attaching SMMs to this junction, MTJ is transformed

into an MTJMSD (Fig. 1(b)), where the SMM molecules form a molecular bridge between the two electrodes.

To characterize our devices, we conducted transport measurements at both low and room temperatures, as well as vibrating sample magnetometry (VSM) at 100 K on both bare and molecule-treated MTJ samples. Our results reveal a significant enhancement in current at room temperature and a reduction in magnetic moment at 100 K temperature after the molecular treatment, indicating the transformative impact of SMM integration on MTJ performance.

II. EXPERIMENTAL DETAILS

We engineered cross-junction-shaped MTJMSD devices by integrating single-molecule magnets (SMMs) as molecular channels connecting ferromagnetic (FM) and antiferromagnetic (AFM) electrodes in patterned magnetic tunnel junction (MTJ) cross-junction configurations. The materials in MTJs were grown using direct current and radio frequency (RF) magnetron sputtering techniques. A specifically designed SMM molecule (Fig. 1(d)) was employed as the molecular bridge, enabling successful assembly of the MTJMSD devices.

For the transport measurements, the MTJ stack was structured as follows (starting from bottom layer): Ta (5 nm)/NiFe (5 nm)/ AlO_x (2 nm)/FeMn (5 nm)/Ta (5 nm), deposited on a silicon wafer with a 300 nm layer of silicon dioxide. The tantalum layer was deposited using direct current sputtering, while the remaining layers were deposited using RF sputtering from stoichiometric targets. The FeMn alloy, with an atomic composition of 50:50 (Fe/Mn), served as the AFM layer. The bottom and top tantalum layers act as wet and capping layer respectively.

The fabrication of MTJMSD involved several stages: (i) photolithography to define the bottom electrode geometry; (ii) growth of bottom electrode layers consisting of Ta and NiFe; (iii) lift-off to remove excess material; (iv) lithography to create the insulating layer and form the cavity for the top electrode; (v) deposition of AlO_x ,

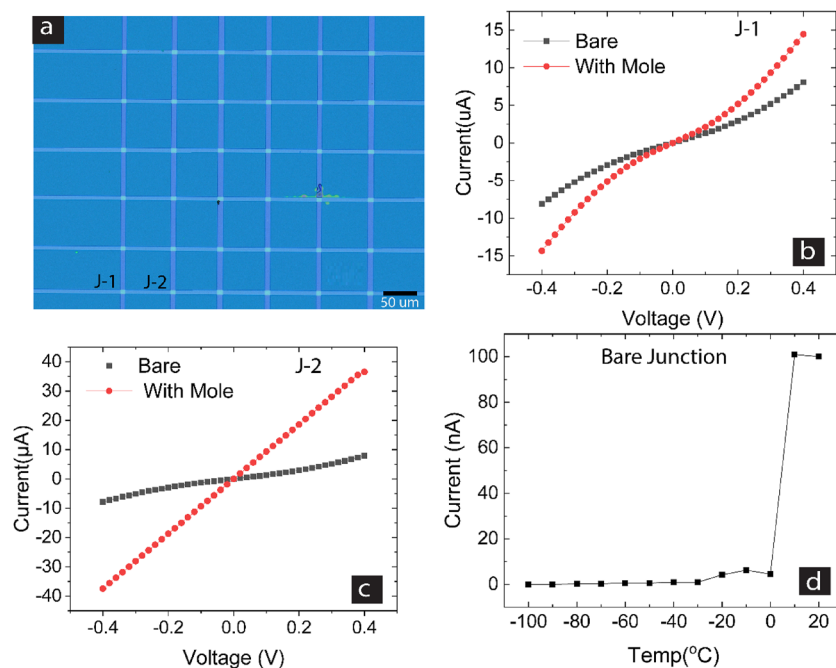


FIG. 2. (a) Photography of the MTJ devices with 36 junctions. Current as a function of voltage for bare and molecule-treated samples at room temperature (b) Junction 1 (J-1), (c) Junction 2 (J-2). (d) Current versus temperature for the bare junction (J-1) at 40 mV biased voltage.¹⁹

the top FeMn antiferromagnet, and capping layers; and (vi) attachment of SMM to MTJ via electrochemical procedure (Fig. 1(b)).²⁰ Figure 2(a) shows an optical microscopy image of the device, which includes 36 cross-junctions with each junction covering an approximate area of $20 \mu\text{m}^2$. A 2D atomic force microscopy image of a single cross-junction, showing the morphological structure of distinct AFM and FM electrodes, is provided in Fig. 1(c). Additional details about the fabrication and molecule attachment process are available in Refs. 16 and 20–22.

III. RESULTS AND DISCUSSION

Two specific junctions of the fabricated cross-junction-shaped MTJ device were characterized using transport measurements at room temperature, both before and after treatment with single-molecule magnets (SMMs). Herein, Figs. 2(b) and 2(c) present current voltage (I-V) measurements for two junctions, labeled Junction 1 (J-1) and Junction 2 (J-2), with black data representing the bare MTJ state and red data representing the MTJ after SMM treatment. In their untreated (bare) state, both MTJ junctions displayed strong tunneling behavior, with leakage currents below the microampere range at low bias voltage of around ~ 50 mV, indicating high-quality AlO_x insulation between the electrodes. A more comprehensive study involving multiple junction measurements has been previously published.¹⁹

In both junctions, electron transport across the electrodes increased to varying degrees after SMM attachment. Initially, the current in the bare state was $\sim 5 \mu\text{A}$ at 400 mV for both J-1 and J-2. After molecule treatment, the current showed discrete levels of enhancement: for J-1, it increased threefold, from $\sim 5 \mu\text{A}$ to $\sim 15 \mu\text{A}$ at 400 mV, while retaining the device's non-ohmic tunneling behavior (Fig. 1(b)). For J-2, the current exhibited an eightfold increase,

rising from $\sim 5 \mu\text{A}$ to $\sim 40 \mu\text{A}$ at the same potential, and the I-V relationship became linear. This current enhancement may result from the unique ability of the SMM to bridge the two magnetic electrodes, altering the magnetic order of both the top and bottom electrodes.¹⁹ Moreover, the SMM's molecular channel between the FM and AFM electrodes contributes to spin filtering²³ and increased spin polarization, further enabling spin dependent electron transport across the channel. This induced spin polarization by SMM points to the potential for future magneto-transport study for comprehensive exploration of these effects.

Compared to conventional AlO_x insulation, an SMM channel can reduce spin scattering due to its robust antiferromagnetic and ferromagnetic coupling with the electrodes, which promotes more coherent spin transport.^{1,13} Interestingly, this current-enhancing effect after molecule attachment differs from previous MTJ studies using dual ferromagnetic electrodes, where SMM treatment actually led to current suppression.¹⁴ This observed contrast suggests that the unique interactions between molecular channels and specific MTJMSD electrode combinations arise from distinct spin orientations and coupling effects, as explored in our earlier theoretical work.¹⁸

To further investigate material properties, we performed low-temperature transport measurements on the MTJ system, ranging from 20°C down to -100°C at a bias of 40 mV (Fig. 2(d)). For the bare MTJ, current remained steady around 100 nA until near 0°C , where it sharply decreased to the picoampere range, stabilizing at this magnitude beyond this critical temperature. This pronounced current suppression at low temperatures (i.e., at 173 K, $\sim -100^{\circ}\text{C}$) is markedly greater than that observed in SMM-treated MTJs reported elsewhere.¹⁹ The extracted data at 40 mV are summarized in Table I, highlighting that the two bare junctions (J-1 and J-2) exhibit pronounced current suppression to the picoampere range at -100°C .

TABLE I. Current at 40 mV for bare and SMM-treated junctions at two different temperatures, measured for two distinct junctions.

Junction	Temperature			
	25°C		−100°C	
	Bare (μA)	With SMM (μA)	Bare (pA)	With SMM (μA)
J-1	~ 0.15	~ 1.01	~ 2.2	~ 0.10
J-2	~ 0.57	~ 3.62	~ 0.76	~ 0.23

In contrast, the SMM-treated samples show a relatively modest suppression of only about 10-fold. Unfortunately, we could not obtain current data across the full temperature range (20°C to −100°C) for the SMM-treated sample due to long-term material degradation.

The exact mechanism behind this current suppression remains unclear, though we surmise that antiferromagnetic materials like FeMn, with a Néel temperature near room temperature, experience increased antiferromagnetic ordering as temperature decreases, significantly impacting conductivity. Below the Néel temperature, antiferromagnetic materials like FeMn might go through a metal-to-insulator transition, which could significantly impact their conductivity.²⁰ Additionally, the capping tantalum layer might change the magnetic properties of the electrodes, further impacting the overall conductivity.^{22,24} Both factors likely contribute to the variations in current that observed in our experiments.

To further explore the effect of the molecule on the MTJMSD system, we conducted magnetization measurements at a low temperature of 100 K. This temperature was opted to reduce the impact of any possible high-temperature transitions in the antiferromagnetic material of MTJMSD. To facilitate these measurements, we fabricated cylindrical pillar-shaped devices using the same material stack as in the cross-junction devices described above. Detailed fabrication procedures are presented in the Ref. 15. Each 4 × 4 mm² fabricated sample piece contained thousands of MTJs, with individual dimensions of five microns and ~10-micron spacing between neighboring pillars, allowing for high-yield insights into the effects of SMM treatment.

Magnetic moment measurements were carried out under an in-plane applied magnetic field ranging from −1000 Oe to 1000 Oe at 100 K, presented as magnetic hysteresis curves in Fig. 3(a) for

both untreated (black data s) and SMM-treated samples (red data). These measurements were conducted using a Quantum Design VersaLab Vibrating Sample Magnetometer (VSM). A noticeable reduction in magnetic moment was observed at low temperatures following the molecular treatment (Fig. 3(a)), aligning with previous findings on MTJMSDs using a Pd/AlO_x/NiFe material stack, suggesting that we can indeed produce MTJMSDs with a high success rate.

We are uncertain about the exact physical phenomena responsible for the reduction in magnetic moment, despite the observed enhancement in transport current. However, theoretical studies on MTJMSDs suggest that molecules can promote robust, long-range antiferromagnetic exchange coupling with both electrodes, potentially altering the spin arrangements within each electrode.¹² This coupling effect may influence the spin density of states in each electrode at 100 K, thereby affecting the magnetic moment. We surmise that such variations in the density of states could alter the position of Fermi level and, consequently, the conductivity observed in our transport measurements (Figs. 2(b) and 2(c)). The alignment of the Fermi level between the electrodes with that of the molecule might explain the non-linearity in the I-V plot (red data points in Fig. 2(c)) after the molecule treatment.

To validate the accuracy of the VSM measurement and rule out any impact of the molecule on a blank wafer, we performed control experiments on a similarly sized (4 × 4 mm²) blank thermally oxidized silicon wafer before and after molecule treatment (Fig. 3(b)). The agreement between the datasets for the untreated (black data) and molecule-treated (red data) blank wafers affirmed a consistent diamagnetic response that bolstered the reliability of our magnetic measurement results and highlighting the specific impact of SMM on the MTJMSD.

IV. CONCLUSION

In this study, we engineered magnetic tunnel junctions (MTJs) using a unique combination of ferromagnetic (NiFe) material as the top electrode and antiferromagnetic (FeMn) materials as the bottom electrode. Integrating single molecule magnets (SMMs) to these MTJs, successfully transformed them into molecular spintronics devices (MTJMSDs). Detailed Transport measurements and vibration sample magnetometry (VSM) studies were conducted to investigate the impact of SMMs on these devices.

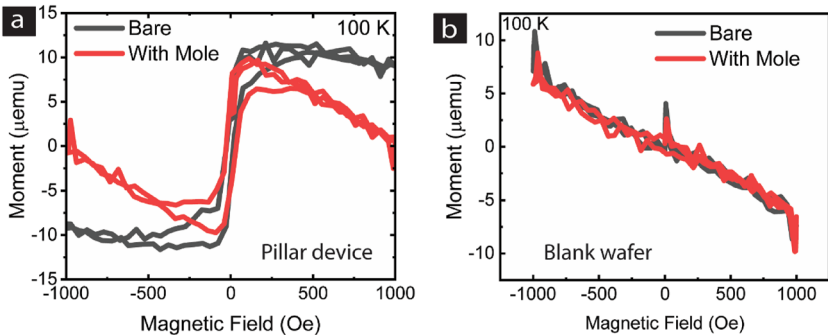


FIG. 3. Magnetic moment as a function of in-plane external magnetic field measured at 100 K. temperature (a) pillar-shaped devices; (b) blank wafer. Black data points represent the bare sample, while red data points represent the SMM molecule-treated sample.

Transport measurement results revealed a significant increase in current after SMM treatment, with the values reaching up to eight times those of untreated MTJ junctions. This enhancement hinted that SMMs efficiently formed a molecule channel between the electrodes facilitating spin dependent electron transport. Additionally, at low temperature, the bare MTJ showed substantial decrease in current (\sim pA) with the decrement more pronounced than molecule treated sample. Furthermore, the VSM measurements at 100 K indicated a reduction in magnetic moment following molecule treatment, emphasizing the influence of SMMs on the magnetic ordering of electrodes.

Our experimental results are crucial in optimizing material combinations for MTJMSDs and demonstrate the potential significance of encompassing antiferromagnetic materials, which offers the benefit of low stray field and zero net magnetization. This work paves the way for the captivating possibilities for the next generation, low-power memory and data storage technologies that utilize molecular spin channels for enhanced performance and efficiency.

ACKNOWLEDGMENTS

We gratefully acknowledge the funding sources; National Science Foundation CREST Award, grant number HRD- 1914751, NSF-MRI grant 1920097, Department of Energy/National Nuclear Security Agency (DE-FOA-0003945) and NASA MUREP Institutional Research Opportunity Grant under Cooperative Agreement #80NSSC19M0196.

AUTHOR DECLARATIONS

Conflict of Interest

The authors have no conflicts to disclose.

Author Contributions

Babu Ram Sankhi: Data curation (equal); Formal analysis (equal); Investigation (equal); Methodology (equal); Writing – original draft (equal). **Erwan Peigney:** Methodology (equal). **Hayden Brown:** Methodology (equal). **Pius Suh:** Methodology (supporting). **Carlos Rojas-Dotti:** Writing – review & editing (equal). **José Martínez-Lillo:** Writing – review & editing (equal). **Pawan Tyagi:** Conceptualization (equal); Project administration (equal); Resources (equal);

Software (equal); Supervision (equal); Writing – review & editing (equal).

DATA AVAILABILITY

The data that support the findings of this study are available from the corresponding author upon reasonable request.

REFERENCES

- ¹L. Bogani and W. Wernsdorfer, *Nat. Mater.* **7**(3), 179–186 (2008).
- ²A. R. Rocha, V. M. Garcia-Suarez, S. W. Bailey, C. J. Lambert, J. Ferrer, and S. Sanvito, *Nat. Mater.* **4**(4), 335–339 (2005).
- ³A. N. Pasupathy, R. C. Bialczak, J. Martinek, J. E. Grose, L. A. Donev, P. L. McEuen, and D. C. Ralph, *Science* **306**(5693), 86–89 (2004).
- ⁴M. N. Leuenberger and D. Loss, *Nature* **410**(6830), 789–793 (2001).
- ⁵J. Petta, S. Slater, and D. Ralph, *Phys. Rev. Lett.* **93**(13), 136601 (2004).
- ⁶P. Tyagi, *J. Mater. Chem.* **21**(13), 4733–4742 (2011).
- ⁷A. Cornia, A. F. Costantino, L. Zobbi, A. Caneschi, D. Gatteschi, M. Mannini, and R. Sessoli, *Single-Molecule Magnets and Related Phenomena* (2006), pp. 133–161.
- ⁸E. Coronado, A. Forment-Aliaga, A. Gaita-Ariño, C. Giménez-Saiz, F. M. Romero, and W. Wernsdorfer, *Angew. Chem.* **116**(45), 6278–6282 (2004).
- ⁹O. Pieper, T. Guidi, S. Carretta, J. Van Slageren, F. El Hallak, B. Lake, P. Santini, G. Amoretti, H. Mutka, M. Koza *et al.*, *Phys. Rev. B* **81**(17), 174420 (2010).
- ¹⁰S. Bahr, C. J. Milios, L. F. Jones, E. K. Brechin, V. Mosser, and W. Wernsdorfer, *Phys. Rev. B* **78**(13), 132401 (2008).
- ¹¹B. R. Dahal, M. Savadkoobi, A. Grizzle, C. D'Angelo, V. Lamberti, and P. Tyagi, *Sci. Rep.* **12**(1), 5721 (2022).
- ¹²A. Grizzle, C. D'Angelo, J. Martínez-Lillo, and P. Tyagi, *RSC Adv.* **11**(51), 32275–32285 (2021).
- ¹³A. Grizzle, C. D'Angelo, and P. Tyagi, *AIP Adv.* **11**(1), 015340 (2021).
- ¹⁴M. Savadkoobi, C. D'Angelo, A. Grizzle, B. Dahal, and P. Tyagi, *Org. Electron.* **102**, 106429 (2022).
- ¹⁵P. Tyagi and E. Friebe, *J. Magn. Magn. Mater.* **453**, 186–192 (2018).
- ¹⁶M. Savadkoobi, D. Gopman, P. Suh, C. Rojas-Dotti, J. Martínez-Lillo, and P. Tyagi, *ACS Appl. Electron. Mater.* **5**(6), 3333–3339 (2023).
- ¹⁷G. Hu, M. Zuo, Y. Li, J. Ren, and S. Xie, *Appl. Phys. Lett.* **104**(3), 033302 (2014).
- ¹⁸E. Mutunga, C. D'Angelo, and P. Tyagi, *Sci. Rep.* **13**(1), 16201 (2023).
- ¹⁹B. Ram Sankhi, E. Peigney, H. Brown, P. Suh, C. Rojas-Dotti, J. Martínez-Lillo, and P. Tyagi, *J. Magn. Magn. Mater.* **611**, 172608 (2024).
- ²⁰P. Tyagi, C. Riso, and E. Friebe, *Org. Electron.* **64**, 188–194 (2019).
- ²¹P. Tyagi, C. Riso, U. Amir, C. Rojas-Dotti, and J. Martínez-Lillo, *RSC Adv.* **10**(22), 13006–13015 (2020).
- ²²P. Tyagi, C. Baker, and C. D'Angelo, *Nanotechnology* **26**, 305602 (2015).
- ²³P. N. Abufager, R. Robles, and N. Lorente, *J. Phys. Chem. C* **119**(22), 12119–12129 (2015).
- ²⁴P. Tyagi and T. Goulet, *MRS Commun.* **8**(3), 1024–1028 (2018).